soma (absence of vacuolar inclusions and exclusion of 0.25% trypan blue). Determinations of the number of viable pyramidal neurons were performed in triplicate 16-mm tissue culture wells; five 1.5-mm^2 fields were scored per well. At least 10 neurons per field or 50 neurons per well were counted in control cultures.
6. S. A. Moody, H. S. Quigg, A. Frankfurter, *J. Comp. Neurol.* **279**, 567 (1989); A. Caceres, G. A. Banker, L. I. Binder, *J. Neurosci.* **6**, 714 (1986). Hippocampal cultures were fixed, preincubated with 5% bovine serum albumin in phosphate-buffered saline and then incubated for 3 hours at 37°C with 1:100 dilutions of monoclonal antibodies (Tu-J1 to neuron-specific class III β tubulin isotype and AP14 to MAP-2). The cultures were then incubated with a biotinylated rabbit antibody to mouse immunoglobulin G followed by ExtrAvidin-Peroxidase (Sigma) and reacted with diaminobenzidine. Cultures treated the same but without primary antibody did not show significant immunoreactivity.
7. Amyloid peptides were synthesized by the solid-phase fluorenylmethoxycarbonyl method on a Milligen peptide synthesizer and purified by reversed-phase high-pressure liquid chromatography on C18 columns. The sequences were confirmed with an Applied Biosystems Model 470 sequencer. The β1-16 and APP676-695 peptides were from Multiple Peptide Systems (San Diego, CA); purity and primary sequences were confirmed. Purified tachykinin peptides were from Bachem, Inc. (Torrance, CA). Lyophilized amyloid peptides were solubilized in 35% acetonitrile, 0.1% trifluoroacetic acid. In this solution, β1-40 did not exhibit aggregation on elution from a C18 column or on 10 to 20% SDS-polyacrylamide gels. Peptide solutions were diluted at least 1:50 directly into culture medium. At this dilution, the vehicle had no detectable effects on neuronal viability or process outgrowth.
8. C. G. Dotti, C. A. Sullivan, G. A. Banker, *J. Neurosci.* **8**, 1454 (1988).
9. B. A. Yankner, *Neurology* **40** (2), 20 (1990).
10. Normalization of values relative to the maximal β1-40–induced change in neuronal number was performed as follows: % trophic response = $\beta - C/\beta_{max} - C \times 100$ and % toxic response = $C - \beta/C - \beta_{max} \times 100$, where β = mean neuronal number in cultures treated with the indicated peptide, β_{max} = mean neuronal number in cultures treated with the maximal (saturating) concentration of β1-40 [day 1, 125 neurons per well (range, 85 to 150); day 5, 35 neurons per well (range, 21 to 50)], C = mean neuronal number in control cultures without peptide [day 1, 78 neurons per well (range, 55 to 110); day 5, 65 neurons per well (range 50 to 75)]. Values are the mean from two to four experiments as indicated. Absence of an increase in neuronal number relative to controls at day 1 and absence of a decrease at day 5 were designated as 0% trophic and toxic responses, respectively.
11. J. Kang *et al.*, *Nature* **325**, 733 (1987).
12. G. H. Beaven, W. B. Gratzer, H. G. Davies, *Eur. J. Biochem.* **11**, 37 (1969).
13. M. O. Dayhoff, R. M. Schwartz, B. C. Orcutt, in *Atlas of Protein Sequence and Structure*, M. O. Dayhoff, Ed. (National Biomedical Research Foundation, Silver Spring, MD, 1978), vol. 5, suppl. 3, pp. 345–352. Tachykinin sequences were from V. Espramer, [*Trends Neurosci.* **4**, 267 (1981)]. Using the log odds matrix for computing relationships between sequences, we compared β25-35 to eledoisin. The calculated probability that the two peptides are related is 1600 times greater than would be predicted by chance alone.
14. R. A. Nicoll *et al.*, *Annu. Rev. Neurosci.* **3**, 227 (1980); R. Quirion and T.-V. Dam, *Regul. Peptides* **22**, 18 (1988); N. Aronin, R. Coslovsky, S. Leeman, *Annu. Rev. Physiol.* **48**, 537 (1986); D. G. Payan, *Annu. Rev. Med.* **40**, 341 (1989).
15. G. Engberg *et al.*, *Nature* **293**, 222 (1981).
16. J. S. Whitson *et al.*, *Neurosci. Lett.* **110**, 319 (1990).
17. D. W. Choi, M. Maulucci-Gedde, A. R. Kriegstein, *J. Neurosci.* **7**, 357 (1987); M. P. Mattson, P. Dou, S. B. Kater, *ibid.* **8**, 2087 (1988).
18. C. M. Lee, N. J. Campbell, B. J. Williams, L. L. Iverson, *Eur. J. Pharmacol.* **130**, 209 (1986); J. E. Maggio, *Annu. Rev. Neurosci.* **11**, 13 (1988).
19. P. W. Mantyh, T. Gates, C. R. Mantyh, J. E. Maggio, *J. Neurosci.* **9**, 258 (1989); T.-V. Dam *et al.*, *Proc. Natl. Acad. Sci. U.S.A.* **87**, 246 (1990).
20. J. K. Mai, P. H. Stephens, A. Hopf, A. C. Cuello, *Neuroscience* **17**, 709 (1986).
21. B. J. Quigley and N. Kowal, *ibid.*, in press.
22. We thank A. Caceres for assistance and P. Lansbury for providing the β34-42 peptide; L. Villa-Komaroff for encouragement and support; and M. Chen, P. Fraser, E. Lamperti, and P. Tempst for discussion. Supported by NIH grants NS01240 (B.A.Y.) and AG08572 (D.A.K.), NSF grant BNS8719741 (L.K.D.), and grants from the Alzheimer's Association (B.A.Y. and L.K.D.) and American Health Assistance Foundation (D.A.K.).

18 April 1990; accepted 7 August 1990

In Vitro Reconstruction of the Respiratory Central Pattern Generator of the Mollusk *Lymnaea*

N. I. SYED, A. G. M. BULLOCH, K. LUKOWIAK

Most rhythmic behaviors such as respiration, locomotion, and feeding are under the control of networks of neurons in the central nervous system known as central pattern generators (CPGs). The respiratory rhythm of the pond snail *Lymnaea stagnalis* is a relatively simple, CPG-based behavior for which the underlying neural elements have been identified. A three-neuron network capable of generating the respiratory rhythm of this air-breathing mollusk has been reconstructed in culture. The intrinsic and network properties of this neural ensemble have been studied, and the mechanism of postinhibitory rebound excitation was found to be important for the rhythm generation. This in vitro model system enables a better understanding of the neural basis of rhythm generation.

DETAILED KNOWLEDGE OF THE neurons that make up CPGs is critical to understanding the neural basis of rhythm generation in both vertebrates and invertebrates. Although in situ recordings can identify specific neurons involved in a behavior, an ideal approach for elucidating the intrinsic and network properties of a neural ensemble is to attempt to reconstruct the circuit in culture. Such a feat is probably impossible for higher animals but might be feasible for adult invertebrates. For instance, mollusks have large identifiable neurons that can be removed from ganglia and maintained in vitro, where they exhibit neurite outgrowth and synapse formation (*1*). Some partial circuits of neurons have been reconstructed in culture (*2–4*), but none of these were involved in rhythm generation.

The aim of this study is to develop an in vitro model system for testing the necessity, appropriateness, and sufficiency of individual components of a respiratory neuronal network in the freshwater pond snail *Lymnaea stagnalis*. Understanding the neural basis of respiratory behavior in this snail may help to determine how similar behaviors are controlled in vertebrates, particularly in diving mammals. *Lymnaea* is a pulmonate mollusk, which, like diving mammals, makes periodic visits to the water surface in order to replenish its air supply. Unlike the opisthobranch mollusks (for example, *Aplysia*) that respire via gills, the pulmonates have lungs. A respiratory orifice termed the pneumostome links the lung cavity with the external environment. Upon reaching the water surface, the pneumostome opens (expiration) and closes (inspiration) several times before the animal resubmerges (*5*). In isolated and semi-intact preparations of *Lymnaea*, this respiratory rhythm is thought to be under the control of two identified interneurons, Input 3 (I.P3.I) and Visceral Dorsal 4 (V.D4) (Fig. 1, A and B), controlling expiration and inspiration, respectively. These respiratory interneurons have reciprocal inhibitory connections with each other and synapse with the appropriate motor neurons that control pneumostome opening and closing (*6, 7*). A third interneuron, the giant dopamine cell of the right pedal ganglion (R.Pe.D1) (Fig. 1, A and B), also appears to be involved in the circuit since it causes the excitation of I.P3.I by postinhibitory rebound (PIR) excitation (*8–10*). Activation of I.P3.I in turn excites the giant dopamine cell while inhibiting V.D4 (*11*). Upon release from I.P3.I inhibition, V.D4 fires and a cycle of alternating bursts is initiated. The giant dopamine cell and V.D4 also have reciprocal inhibitory connections (Figs. 1B and 3A). In this study we show that these three interneurons are sufficient to account for the respiratory rhythms in vitro (Fig. 3B).

The circuitry underlying rhythmic respiratory behavior in *Lymnaea* (Fig. 1B) has features in common with the "half center model" whereby two groups of neurons

Neuroscience Research Group and Department of Medical Physiology, Health Sciences Center, University of Calgary, Calgary, AB T2N 4N1 Canada.

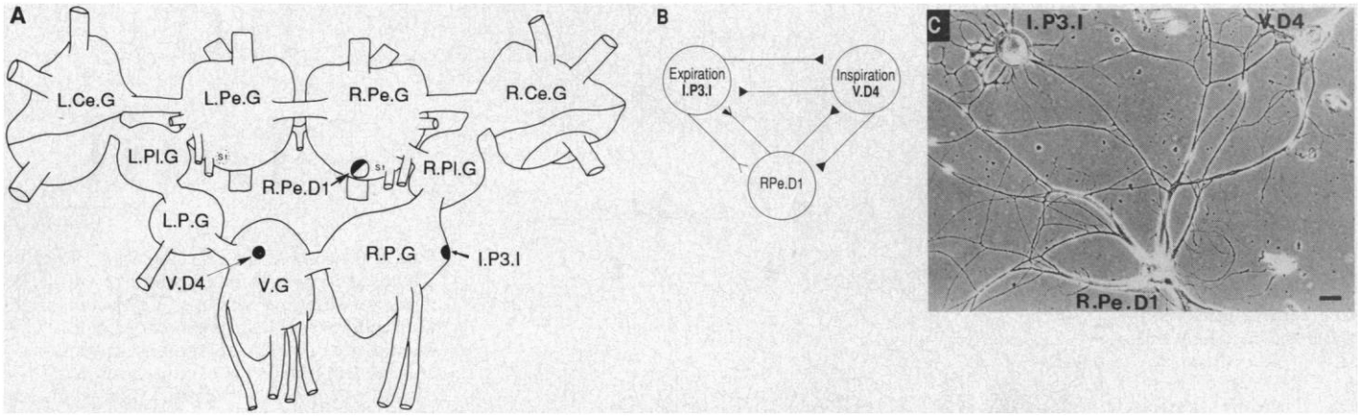

Fig. 1. (**A**) Schematic diagram of the central ganglionic ring of the snail *L. stagnalis* (dorsal view). The central ganglionic ring consists of paired left and right cerebral ganglia (L.Ce.G and R.Ce.G); left and right pedal ganglia (L.Pe.G and R.Pe.G); left and right pleural ganglia (L.Pl.G and R.Pl.G); left and right parietal ganglia (L.P.G and R.P.G); and an unpaired visceral ganglion (V.G). The giant dopamine cell (R.Pe.D1) and Visceral Dorsal 4 (V.D4) are located on the dorsal surfaces of the right pedal ganglion and visceral ganglion, respectively. The Input 3 Interneuron (I.P3.I), on the other hand, which has only recently been identified (*7*), is located on the ventrolateral surface of the right parietal ganglion; St, statocyst. (**B**) Summary diagram showing the in vivo connections between the respiratory interneurons (I.P3.I and V.D4) and the giant dopamine cell (R.Pe.D1). Stimulation of R.Pe.D1 excites I.P3.I by a mixed inhibitory-excitatory connection, which in turn causes the opening of the pneumostome coupled with expiration. Once activated by R.Pe.D1, the I.P3.I excites R.Pe.D1 while inhibiting V.D4. Interneuron V.D4 then recovers from the inhibitory effects of I.P3.I and fires a burst of action potentials, causing the closure of the pneumostome, which constitutes the inspiratory phase of respiration. Both V.D4 and R.Pe.D1 have reciprocal inhibitory connections (see also Fig. 3). (△, Excitatory connection; ▲, inhibitory connection.) (**C**) Photomicrograph of the respiratory interneurons and giant dopamine cell cultured in vitro for 24 hours. The giant dopamine cell and the respiratory neurons were isolated from their respective ganglia [see (A)]. We adopted already established techniques (*20, 21*) for culture of identified *Helisoma* neurons to *Lymnaea* neurons with modifications (*22*). Calibration bar = 100 μm.

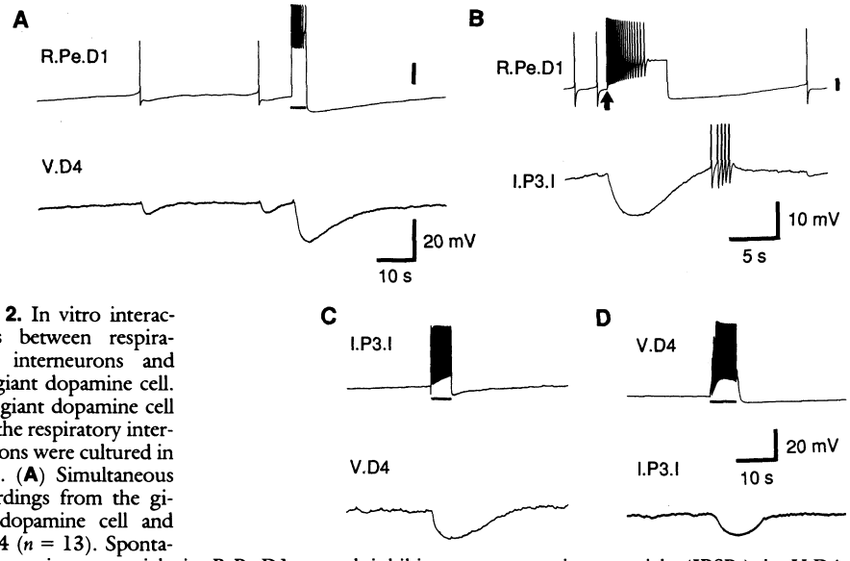

Fig. 2. In vitro interactions between respiratory interneurons and the giant dopamine cell. The giant dopamine cell and the respiratory interneurons were cultured in pairs. (**A**) Simultaneous recordings from the giant dopamine cell and V.D4 (n = 13). Spontaneous action potentials in R.Pe.D1 caused inhibitory postsynaptic potentials (IPSPs) in V.D4. Similarly, depolarization of the giant dopamine cell (at bar) caused a large summated IPSP in V.D4. (**B**) Dual recordings from the giant dopamine cell and I.P3.I (n = 10). A burst of action potentials was elicited in the giant dopamine cell by depolarizing current injection (at arrow). After recovery from inhibition by the giant dopamine cell, I.P3.I exhibited a PIR burst of action potentials. Spontaneous action potentials in the giant dopamine cell induced unitary IPSPs in I.P3.I. (**C** and **D**) Both I.P3.I and V.D4 had reciprocal inhibitory connections with each other, but in both cases the inhibition did not result in the activation of these neurons by PIR excitation (n = 10 to 15). The bursts were driven by current injection at bars (range of currents tested 0.2 to 0.5 nA).

with antagonistic motor functions reciprocally inhibit each other in a cyclical manner (*12*). This model has been proposed to account for many rhythmic behaviors in both vertebrates and invertebrates (*13–15*), but few direct tests of the model have been attempted. Even in semi-intact or isolated brain preparations of *Lymnaea*, it is difficult to demonstrate unequivocally that the giant dopamine cell and the respiratory interneurons are sufficient to account for the respiratory rhythm. In order to test their intrinsic and network properties, we isolated the three interneurons and cultured them in vitro (Fig. 1C). In performing these experiments, we looked for, but did not observe, any obvious changes of neuronal properties due to axotomy or culture procedures (*16*).

Each of the cultured interneurons exhibits extensive neurite outgrowth within 18 to 24 hours (Fig. 1C) when plated in brain-conditioned medium (*17*), and each makes synaptic connections similar to those observed in vivo. In all cases the chemical synapses between any pair of neurons were appropriate; that is, they were of the same type found in vivo. For example, interneuron V.D4 always formed an inhibitory synapse both on the I.P3.I (Fig. 2D) and the giant dopamine cell (not shown), and I.P3.I and the dopamine cell always formed inhibitory synapses on V.D4 (Fig. 2, A and C).

Since the data obtained from both semi-intact and isolated brain preparations showed that the respiratory interneurons were usually quiescent and fired bursts of action potentials only during an active respiratory cycle (*11*), it seemed probable that none of these neurons were endogenous bursters. The intrinsic properties of the cultured neurons were therefore examined. The giant dopamine cell was spontaneously active, and the injection of depolarizing current only increased its firing frequency (Fig. 2, A and B). When cultured either as single cells or in pairs, the respiratory interneurons were quiescent. Depolarizing current injection into either of the cells elicited only a

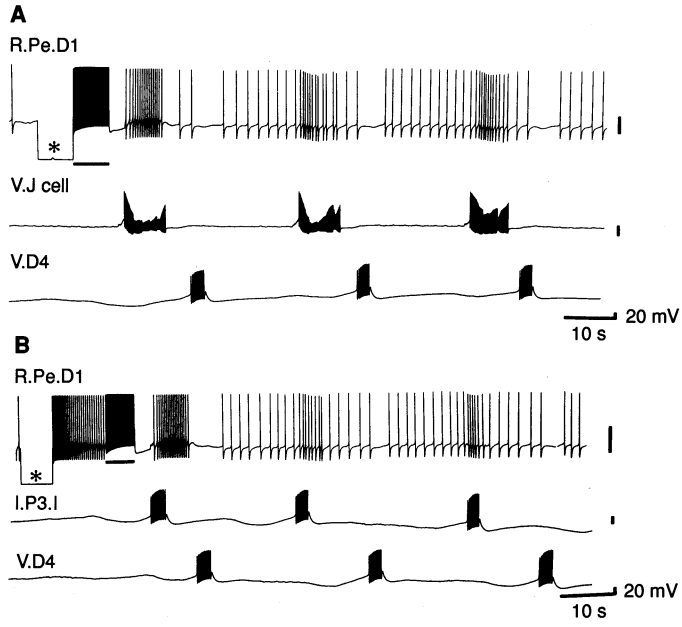

Fig. 3. Intracellular recordings from respiratory interneurons and the giant dopamine cell recorded (A) in situ and (B) in vitro. (**A**) Stimulated respiratory rhythm recorded from the isolated brain preparation. Because of the difficulties in recording intracellular activity simultaneously from both the respiratory interneurons and the giant dopamine cell (I.P3.I is oriented toward the ventral side of the right parietal ganglion whereas R.Pe.D1 and V.D4 are located on the dorsal surface), indirect evidence for the occurrence of I.P3.I was obtained from its follower, Visceral J cell (V.J cell) (*6*). Direct recordings were made from R.Pe.D1 and V.D4. Injection of hyperpolarizing current into R.Pe.D1 (asterisk) revealed lack of passage of hyperpolarizing current between these interneurons. Detailed analysis of this three-cell circuit both in vivo and in vitro also showed lack of electrical coupling between these neurons (not shown). In contrast, when depolarizing current was injected into R.Pe.D1 (at bar), it initiated the I.P3.I activity (as recorded from V.J cell) while inhibiting V.D4. The activation of I.P3.I in turn excited the giant dopamine cell and the previously hyperpolarized V.J cell while inhibiting V.D4. Upon recovery from inhibition by I.P3.I, V.D4 fired a burst of action potentials, and the cycle was spontaneously repeated. (**B**) Both the respiratory interneurons and the giant dopamine cell were isolated in culture and were allowed to extend neurites for 24 hours. These cells were then impaled with glass microelectrodes, and simultaneous intracellular recordings were made. The respiratory interneurons were quiescent; the injection of hyperpolarizing current into the R.Pe.D1 (asterisk) revealed a lack of electrical coupling between these cells. Nevertheless, the injection of strong depolarizing current (at bar) inhibited both of the respiratory interneurons. The direct interaction between R.Pe.D1 and V.D4 can be seen more clearly during the train of action potentials that precedes the strong depolarization of R.Pe.D1 (at bar). I.P3.I recovered from this inhibition and fired a burst of action potentials due to the PIR excitation. This activation of I.P3.I in turn excited R.Pe.D1 and caused the further inhibition of V.D4. Similarly, V.D4 recovered from the inhibition by I.P3.I and fired a burst of action potentials inhibiting both R.Pe.D1 and I.P3.I. Thus, an alternating pattern of bursting activity was initiated by R.Pe.D1 that continued for several cycles before reaching a quiescent state (n = 8). This in vitro pattern of activity mimics the respiratory cycle seen in both isolated and semi-intact preparations.

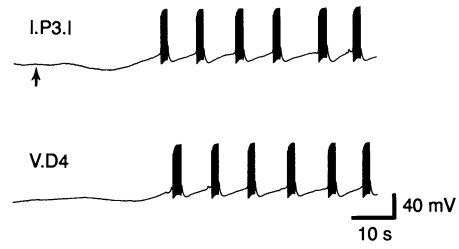

Fig. 4. Dopamine elicited alternating bursts of activity in respiratory interneurons in vitro. The two respiratory interneurons (V.D4 and I.P3.I) were cultured without the giant dopamine cell for 4 days. The mutually inhibitory synapses formed as usual, but stimulation of either neuron did not elicit PIR excitation in its partner (not shown, but see Fig. 3). Phasic application of dopamine (1-s pulses at 0.3 Hz), beginning at the arrow, caused a transient hyperpolarization of both neurons. I.P3.I recovered first from the hyperpolarization with a burst of action potentials, which in turn further inhibited neuron V.D4. Neuron V.D4 then recovered from inhibition and itself produced a burst of action potentials. In this manner, a series of alternating bursts was initiated (seven trials were repeated in three separate preparations). The dopamine (10 μM) was applied via a fire-polished glass pipette; pressure pulses were delivered by a Medical Systems Neurophore BH-2 system.

single burst of action potentials that often outlasted the stimulus, but no repetitive bursting pattern was observed (Fig. 2, C and D). Thus, the rhythm could not be generated intrinsically by any of these neurons alone, since none of them was found to be an endogenous burster.

In order to test whether the respiratory rhythm could be generated by the network properties of the two respiratory interneurons (that is, in the absence of the giant dopamine cell), these cells were cultured and allowed to extend neurites. In all cases (n = 9), intracellular injection of depolarizing current into either of these cells inhibited the other but failed to evoke PIR excitation, which is the basis of the respiratory cycle (Fig. 2, C and D). When the giant dopamine cell was cultured with individual respiratory interneurons, injection of current into this cell did not trigger rhythmic firing, although appropriate inhibitory connections were apparent (Fig. 2, A and B). I.P3.I, but not V.D4, exhibited PIR excitation after inhibition by the giant dopamine cell, in a manner similar to that observed in isolated ganglionic preparations (Fig. 2B).

We next tested whether the respiratory rhythm could be generated when all three interneurons were cultured together. Both I.P3.I and V.D4, as described earlier, were quiescent, but, when depolarizing current was injected into the giant dopamine cell, it inhibited both of these respiratory interneurons (Fig. 3B). However, I.P3.I recovered from this inhibition and fired a burst of action potentials, apparently as a result of PIR excitation. The activation of I.P3.I in turn excited the giant dopamine cell, and the combined activity of these neurons caused PIR excitation of the V.D4 interneuron. Thus I.P3.I and V.D4 began bursting alternately, mimicking the respiratory cycle seen in semi-intact and isolated brain preparations (Fig. 3A). The generation of alternating bursts was observed in all trials in the eight preparations in which the three interneurons were successfully cultured together.

Our experiments suggested that the giant dopamine cell might be necessary for the generation of the respiratory rhythm. We examined this hypothesis by attempting to substitute the giant dopamine cell with other identified neurons of known transmitters. In this context we substituted for the giant dopamine cell either the giant serotonergic neuron of the left pedal ganglion (*18*) or the neuron containing an adrenocorticotropic hormone (ACTH)–like peptide of the visceral ganglion (*19*). In neither of these cases were synaptic connections formed on the respiratory interneurons nor was the respiratory rhythm generated.

Our data suggested that dopamine itself might be necessary for rhythm generation. To test this hypothesis, we cultured the respiratory interneurons together in the absence of the giant dopamine cell. The mutual inhibitory connections developed between the two respiratory interneurons, and dopamine was applied either tonically or via pressure pulses in a fast perfusion system. Tonic application of dopamine (10 μM) caused a prolonged but reversible hyperpolarization of both interneurons. In contrast, phasic application of the same concentration of dopamine (1-s pulses at 0.3 Hz) elicited a series of alternating bursts similar (although of higher frequency) to that exhibited by the three neuron network both in vivo and in vitro (Fig. 4). At present, it is unknown whether the high-frequency burst pattern seen in I.P3.I and V.D4 after the phasic application of dopamine is due to the fre-

quency of the dopamine pressure pulses or to the relative dopamine concentration. The generation of rhythmic bursting by the two interneurons is not a function of the continuous presence of dopamine but rather requires the phasic application of dopamine, which presumably mimics the effects of giant dopamine cell activity.

We have shown that it is possible to culture a neural network that is sufficient to produce rhythmic activity similar to that seen in vivo. It can be argued that networks of neurons constructed in vitro cannot be used to prove that a similar circuit functions in vivo. However, no obvious differences in the excitability and connectivity of the interneurons were apparent between our in vivo and in vitro preparations. The experiments of this report provide evidence that three identified interneurons are sufficient to account for a CPG. Furthermore, dopamine is necessary for rhythm generation in this network. Such tests are impossible to perform in the intact nervous system. Our in vitro model system may provide an opportunity to test the cellular basis of rhythm generation in a manner unapproachable in vivo.

REFERENCES AND NOTES

1. A. G. M. Bulloch, Ed., *Cellular Basis of Neuronal Plasticity*, vol. 7 of *Studies in Neuroscience*, W. Winlow, Series Ed. (Manchester Univ. Press, Manchester, UK, 1989).
2. J. Camardo, E. Proshansky, S. Schacher, *J. Neurosci.* **3**, 2614 (1983).
3. S. G. Rayport and S. Schacher, *ibid.* **6**, 759 (1986).
4. D. Kleinfeld, F. F. Raccuria-Behling, H. J. Chiel, *Biophys. J.* **57**, 697 (1990).
5. J. D. Jones, *Comp. Biochem. Physiol.* **4**, 1 (1961).
6. N. I. Syed and W. Winlow, *J. Physiol. (London)* **403**, 78p (1988).
7. N. I. Syed, R. L. Ridgway, A. G. M. Bulloch, K. Lukowiak, in preparation.
8. W. Winlow, P. G. Haydon, P. R. Benjamin, *J. Exp. Biol.* **94**, 137 (1981).
9. N. I. Syed, D. Harrison, W. Winlow, in preparation.
10. N. I. Syed and W. Winlow, in preparation.
11. N. I. Syed, thesis, University of Leeds, Leeds, United Kingdom (1988).
12. T. G. Brown, *Proc. R. Soc. London Ser. B.* **84**, 308 (1911).
13. A. I. Selverston, Ed., *Model Neural Networks and Behavior* (Plenum, New York, 1985).
14. J. W. Jacklet, Ed., *Neuronal and Cellular Oscillators* (Dekker, New York, 1989).
15. R. Lydic, *FASEB J.* **3**, 2457 (1989).
16. Properties tested include resting membrane potential, action potential amplitude, and wave form.
17. R. G. Wong, R. D. Hadley, S. B. Kater, G. Hauser, *J. Neurosci.* **1**, 1008 (1981).
18. G. Audesirk, *Comp. Biochem. Physiol.* **81A**, 359 (1985).
19. H. H. Boer *et al.*, *Cell Tissue Res.* **202**, 231 (1979).
20. R. D. Hadley, D. A. Bodnar, S. B. Kater, *J. Neurosci.* **15**, 3145 (1985).
21. P. G. Haydon, C. S. Cohan, D. P. McCobb, H. R. Miller, S. B. Kater, *J. Neurosci. Res.* **13**, 135 (1985).
22. Dissected ganglia were treated with a mixture of 0.2% collagenase and dispase (Boehringer Mannheim) and 0.2% trypsin (Sigma type III) in a ratio of 2:1, respectively, for 30 to 40 min in defined medium (7), and then with 0.2% trypsin soybean inhibitor (Sigma) for 10 min, also in defined medium. After microdissection of the outer sheath, inner connective tissue sheaths were removed from the ganglionic ring. Identified neurons were removed via gentle suction with fire-polished pipettes from appropriate ganglia maintained in high-osmolarity medium (defined medium containing 30 mM glucose). Neurons were then transferred to poly-L-lysine-coated Falcon 3001 culture plates containing brain-conditioned medium prepared as described (*20, 21*). The pH of the medium was adjusted to 7.9 with 1 N NaOH.

23. We thank B. MacVicar, R. L. Ridgway, and S. Weiss for critical reviews of the manuscript, T. Stirling for its preparation, and G. Hauser for technical assistance. Supported by grants from the Medical Research Council (Canada). A.G.M.B. is an Alberta Heritage Foundation for Medical Research Scholar.

14 May 1990; accepted 16 August 1990

A Magnesium Current in *Paramecium*

ROBIN R. PRESTON

Recent reappraisals of the role of ionized magnesium in cell function suggest that many cells maintain intracellular free Mg^{2+} at low concentrations (0.1 to 0.7 mM) and that external agents can influence cell function via changes in intracellular Mg^{2+} concentration. Depolarization and hyperpolarization of voltage-clamped *Paramecium* elicited a Mg^{2+}-specific current, I_{Mg}. Both Co^{2+} and Mn^{2+} were able to substitute for Mg^{2+} as charge carriers, but the resultant currents were reduced compared with Mg^{2+} currents. Intracellular free Mg^{2+} concentrations were estimated from the reversal potential of I_{Mg} to be about 0.39 mM. The I_{Mg} was inhibited when external Ca^{2+} was removed or a Ca^{2+} chelator was injected, suggesting that its activation was Ca^{2+}-dependent.

MAGNESIUM HAS LONG BEEN RECognized to be a necessary cofactor for numerous enzymatic reactions (*1*), but there is now considerable evidence to suggest that intracellular free Mg^{2+} ($[Mg^{2+}]_i$) may also be a key physiological regulator of cell activity (*2, 3*). In the past, researchers have been reluctant to consider such a role for Mg^{2+} because it was believed that $[Mg^{2+}]_i$ was of the order of 10 to 30 mM (*1*). Recently, however, techniques have been developed that allow $[Mg^{2+}]_i$ to be measured with accuracy (*4*). These methods suggest that, although total intracellular Mg^{2+} concentration is indeed high, the majority of it exists in a bound form. Intracellular free Mg^{2+} concentration is actually 0.1 to 0.7 mM (*1–3*). Since the Michaelis constant (K_m) values for Mg^{2+} activation or inhibition of many enzymes fall within this range (*1*), relatively small changes in $[Mg^{2+}]_i$ could have large effects on cell activity. Although the short half-life of $^{28}Mg^{2+}$ and the lack of Mg^{2+}-sensitive dyes has hampered attempts to characterize possible $[Mg^{2+}]_i$ regulatory mechanisms, it is

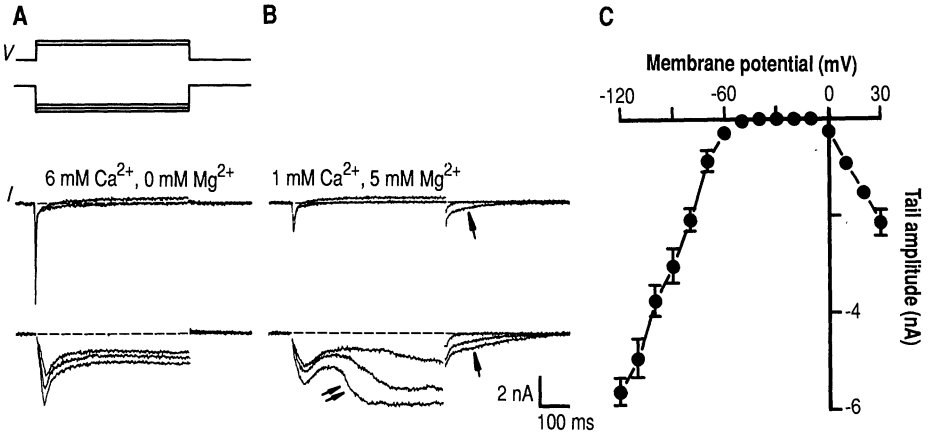

Fig. 1. I_{Mg} in *P. tetraurelia*. (**A**) Voltage steps (*V*) (500 ms) from −30 mV to 10 and 20 mV, or to −80, −90, and −100 mV, were used to elicit currents (*I*). (**B**) Repetition of the voltage steps in (A) after adding 5 mM Mg^{2+} to the bath. Arrows, slow inward tail currents of I_{Mg}. Traces have been corrected for linear leakage current, estimated from repeated small (3 to 9 mV, 20 ms) hyperpolarizations. Broken lines represent holding currents (about −0.2 nA in both Mg^{2+} and Ca^{2+} solutions). (**C**) I_{Mg} tail current amplitudes at the moment of return to the holding potential as a function of membrane potential. Currents activated during the voltage steps contained minor active components in addition to I_{Mg}; thus, studies of I_{Mg} under various conditions usually focused on tail currents. These tails represent pure I_{Mg}: note the lack of similar tail currents in the absence of extracellular Mg^{2+} (Table 1A). Values are means ± SEM from 12 cells.